Journal of the European Ceramic Society 21 (2001) 381–387

www.elsevier.com/locate/jeurceramsoc

Microstructure development in calcium hexaluminate

Cristina Domínguez [a], Jérome Chevalier [a,*], Ramon Torrecillas [b], Gilbert Fantozzi [a]

[a] *INSA GEMPPM-UMR5510, 69621 Villeurbanne Cedex, France*
[b] *INCAR CSIC, Ap. 73 33080 Oviedo, Spain*

Received 27 November 1999; received in revised form 15 April 2000; accepted 29 April 2000

Abstract

Calcium hexaluminate (CA_6) was prepared from alumina and calcium carbonate powders. The influence of processing method and firing temperature on calcium hexaluminate grain morphology was studied. A significant correlation was found between grain morphology and green density, porosity distribution and presence of agglomerates. Platelet grains were observed for low green densities and large pores, while more equiaxed grains were found when green density was increased. A model is proposed for the formation of equiaxed or platelet grains. The model is based on the number of contact areas between alumina and calcium carbonate grains in green specimens as well as on the free space available for calcium hexaluminate to grow. © 2001 Elsevier Science Ltd. All rights reserved.

Keywords: $CaAl_{12}O_{19}$; Grain growth; Grain morphology; Microstructure-final

1. Introduction

Calcium hexaluminate ($CaAl_{12}O_{19}$ or $CaO{\cdot}6Al_2O_3$), often denoted as CA_6, occurs in nature as the mineral hibonite. This phase is the most alumina-rich intermediate compound of the CaO-Al_2O_3 system.[1] It is thermodynamically stable up to the peritectic point, over 1875°C (between 1820 and 1883°C according to the different authors[2]). At the peritectic temperature, it decomposes giving alumina and a melt phase. CA_6 has a theoretical density of 3.79 g/cm^3,[3] crystallizes in the hexagonal system (spacegroup $P6_3/mmc$),[3–5] and presents the structure of magnetoplumbite.

Previous studies[6–9] have shown the following reaction sequence between $CaCO_3$ and Al_2O_3 to form CA_6:

$$CaCO_3 + Al_2O_3 \rightarrow CaO + Al_2O_3 + CO_{2(gas)}$$

$$CaO + Al_2O_3 \rightarrow CaO{\cdot}Al_2O_3$$

$$CaO{\cdot}Al_2O_3 + Al_2O_3 \rightarrow CaO{\cdot}2Al_2O_3$$

$$CaO{\cdot}Al_2O_3 + 4Al_2O_3 \rightarrow CaO{\cdot}6Al_2O_3$$

where the reaction temperatures can vary as a function of grain size, powder dispersion, forming method, etc.

The morphology of CA_6 grains shows preferential growth along their basal plane. Coupled diffusion of Ca^{2+} ions and O^{2-} ions from calcia-rich to alumina-rich phases is thought to control CA_6 formation.[10] This growth-rate anisotropy is responsible both for the orientation of CA_6 with basal planes perpendicular to the reaction front,[10–13] and for the platelike grain morphologies when CA_6 is obtained by reaction sintering.[8,14] On the contrary, when CA_6 is synthesized and milled previously to press and sintered, grains are always equiaxed[14,15] (to classify grain shapes, the terms defined by Song et al.[16] for alumina grains are used). Sometimes CA_6 obtained by reaction sintering can also present equiaxed morphologies.[6,8] At present there is no clear explanation for the formation of CA_6 grains of both morphologies. Recently there has been a renewed interest in the processing of ceramics whose microstructure exhibits platelike morphologies. This has arisen in great part due to the fact that elongated grains can act as bridging sites in the wake of a crack, hence resulting in improved mechanical behavior. Amongst magnetoplumbites that present this kind of morphology, CA_6 has been chosen as a reinforcing material in alumina composites due to both its chemical compatibility with alumina and its mechanical and thermal expansion properties.[8,9,17–20]

* Corresponding author. Tel.: +33-7243-8382; fax: +33-7243-8528.
E-mail address: jerome.chevalier@insa-lyon.fr (J. Chevalier).

0955-2219/01/$ - see front matter © 2001 Elsevier Science Ltd. All rights reserved.
PII: S0955-2219(00)00143-6

Calcium hexaluminate is a reaction product in alumina and alumina-spinel castables that enhances their hot strength.[21–23] It presents a large primary crystallization field in the $CaO–Al_2O_3–Fe_2O_3$ system,[24–26] which means low solubility in iron containing slags. It is also highly stable in reducing atmospheres.[27] These properties allow CA_6 to be in contact with steel and iron at high temperature without significant corrosion of the ceramic material. Its crystallographic basal planes, with perfect cleavage, can be oriented parallel to a fiber-matrix interface: This makes CA_6 a suitable material for alumina fiber coatings.[28–30] Hexaluminates can retain a large surface area at elevated temperature and can be good candidates as support materials for high temperature catalytic processes.[31] Thanks to the capacity of magnetoplumbites to accommodate fission products such as Sr, Ba, Cs, and Ce in their structure, they are good host structures for long term immobilization of nuclear waste.[32–34]

It is necessary to understand the mechanism of formation of CA_6 grains in order to better develop the potential applications of this material. The aim of the present work is to study the influence of processing method on the final microstructure of reaction-sintering calcium hexaluminate.

The effect of alumina and calcium carbonate distribution in green specimens on the final microstructure was studied by modifying porosity and contact areas between alumina and calcium carbonate grains: processing of materials with different degrees of $CaCO_3$ and Al_2O_3 agglomeration modified these two parameters. The presence of these agglomerates can affect microstructure for different reasons:

1. Due to differences in the extension of the contact areas between $CaCO_3$ and Al_2O_3: CA_6 grains start to be formed at contact surfaces. The presence of agglomerates reduces contact areas, and consequently the number of grains formed per unit volume is lower.
2. Due to differences in porosity or free space between grains: agglomeration tends to produce low green densities in a compact and voids with similar size to the original agglomerates.[35] If there is not enough space, grains growth can be blocked by the presence of other grains of the same material.
3. Due to reaction rate differences, that could affect reaction temperatures and hence be responsible of the appearance of a transient liquid phase.

2. Experimental procedure

CA_6 was formed by reaction sintering of a mixture of 85.9 wt.% alumina (CT3000SG, Alcoa, Pittsburgh, PA) and 14.1 wt.% calcium carbonate powders (PG-40, Asturcal, Gijon, Spain). In order to obtain different agglomeration degrees, different processing methods were used. Two slurries were prepared in desionized water medium by mixing alumina and calcium carbonate powders via mechanical stirring for 5 h, or via attrition milling for 1/2 h using 3 mm zirconia ball grinding media. Both slurries were subsequently dried while subjected to continuous mixing on a stirrer/hot plate and finally sieved under 63 μm. Dried powders were cold isostatically pressed at 200 MPa to give SP (Stir + Pressing) and AP (Attrition + Pressing) samples. A third set of samples designated AC (Attrition + slip Casting), was prepared by slip casting from the former slurry mixed by attrition milling. Green samples were fired in air, at 1650 and 1750°C for 5 h.

Different processing routes produced materials with different alumina and calcium carbonate distributions. For example, dispersion is not optimal with mechanical stirring: alumina and calcium carbonate agglomerates of considerable size can be obtained. On the other hand, attrition milling produces well-dispersed powders and agglomeration is drastically reduced.

Bulk density and open porosity of sintered samples were measured by the Archimedes method using distilled water. Sintered samples were cut and polished with a series of diamond pastes down to 1 μm. The polished samples were thermally etched at 1500°C for 1 h and gold coated for scanning electron microscopy observation (SEM) using a Zeiss DSM 942 microscope equipped with an Energy Dispersive X-ray microanalysis (EDX) Link Oxford.

Grain size was measured from SEM micrographs on a minimum of 500 grains, measuring individually the length and width of each grain with an error less than 0.4 μm.

3. Results

Table 1 shows the bulk density and grain size of sintered samples. As already reported in the literature,[6,9,14] it is difficult to reach full density in reaction sintered CA_6: even increasing sintering temperature up to 1750°C, i.e. slightly below the fusion temperature of pure hibonite, the density is only 96% of theoretical density. Materials mixed by mechanical stirring (SP) present lower densities than materials mixed by attrition milling (AC and AP). Density evolution as a function of sintering temperature depends on processing route. The increase in density with firing temperature is more significant in the material processed by attrition and slip casting (AC) than in the other materials, due to differences in porosity distribution (see Fig. 1). It is well known that the tendency of large pores is to grow during a densification process, while small ones shrink and disappear.[35] In low-density specimens (SP), pores have a

Table 1
Processing conditions, density and final microstructure

Sample	Mixing method	Forming method	Firing temperature (°C)	Bulk density (%)	Open porosity (%)	Length (μm)	Width (μm)	Aspect ratio
SP	Stirring	Cold isostatic pressing	1650	73.5±0.1	18.1±0.7	4.2±2.4	1.2±0.8	4.3±3.5
			1750	86.2±0.5	2.8±0.2	6.5±3.5	2.5±1.5	2.9±1.5
AC	Attrition Milling	Slip casting	1650	76.5±0.7	15.6±1.2	3.0±1.7	1.2±0.6	2.6±1.6
			1750	94.6±0.2	0.1±0.1	3.4±1.8	1.5±0.8	2.6±2.1
AP	Attrition Milling	Cold isostatic pressing	1650	89.3±0.1	0.6±0.1	3.4±1.4	1.4±0.5	2.7±1.6
			1750	96.4±0.3	0.1±0.1	3.2±1.9	1.6±0.8	2.2±1.0

wide size distribution and pores size can attain 50 μm. Density increases with firing temperature due to the size reduction of small pores, while bigger pores remains in the microstructure giving a porosity of 12.8% (see Table 1). In AC and AP samples, pores are clearly smaller and are more homogeneously distributed and, thanks to the absence of large pores, the porosity decreases after firing at 1750°C to 5.4%. This is the reason for the higher sinterability of AC compared to SP materials. AP samples present a pore distribution similar to AC but with lower pore volume, and subsequently the decrease in porosity is reduced.

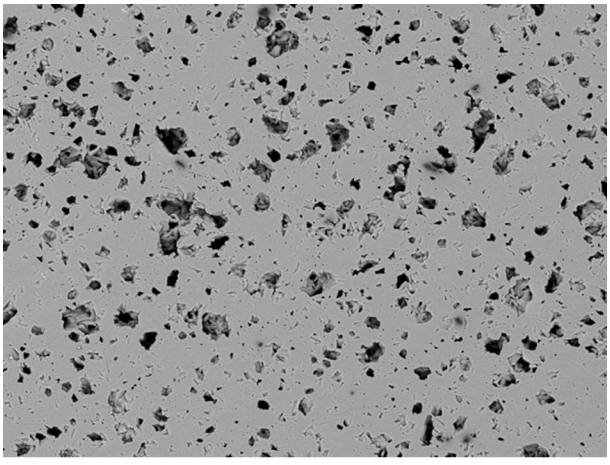

(a)

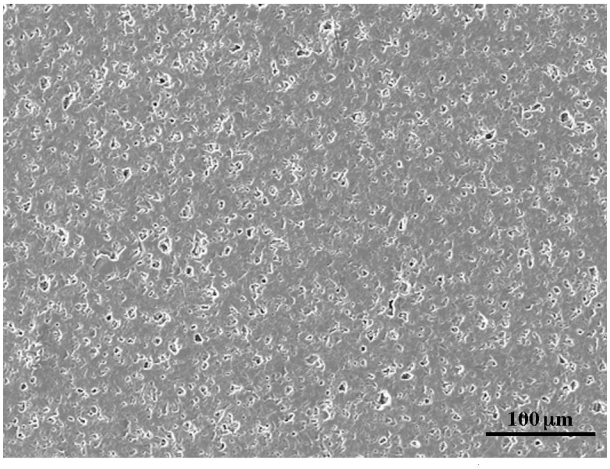

(b)

Fig. 1. SEM low-magnification images of (a) SP and (b) AC samples fired at 1750°C. Note the different porosity size.

Final microstructures of the three materials fired at 1650 and 1750°C are presented in Fig. 2. As can be observed in this figure, only materials mixed by mechanical stirring, which presented big size agglomerates in the green compact, have a clear platelet structure. Grains of SP sample fired at 1650°C have straight boundaries and high aspect ratio showing clear platelet morphology. AC and AP grains present more irregular boundaries and lower aspect ratio showing more equiaxed morphology. In these samples, even if the majority of grains are equiaxed, some platelet grains with lower aspects ratio than SP specimens can be observed. Sample density can be related with grain size as shown in Fig. 3. For samples fired at 1650°C all materials have the same grain width and, except in the case of the material showing lower density, the same grain length and aspect ratio. Nevertheless in the case of the material with lower density, the grain length increases, also increasing the aspect ratio. Materials fired at 1750°C present similar evolution; the larger the grain size the lower the density.

As shown in Table 1, where grain size is plotted as a function of sintering, they are no changes of grain size in the case of materials mixed by attrition milling when sintering temperature is increased from 1650 to 1750°C. Nevertheless, in the case of the material mixed by stirring, there is a grain growth giving a more equiaxed microstructure.

In addition to the fact that platelet grains are obtained only in low-density samples, it is important to point out that in the case of CA_6 equiaxed materials densification is possible at very high temperatures without significant grain coarsening.

4. Discussion

The observed dependence of CA_6 morphology on raw material distribution in green specimens has not been

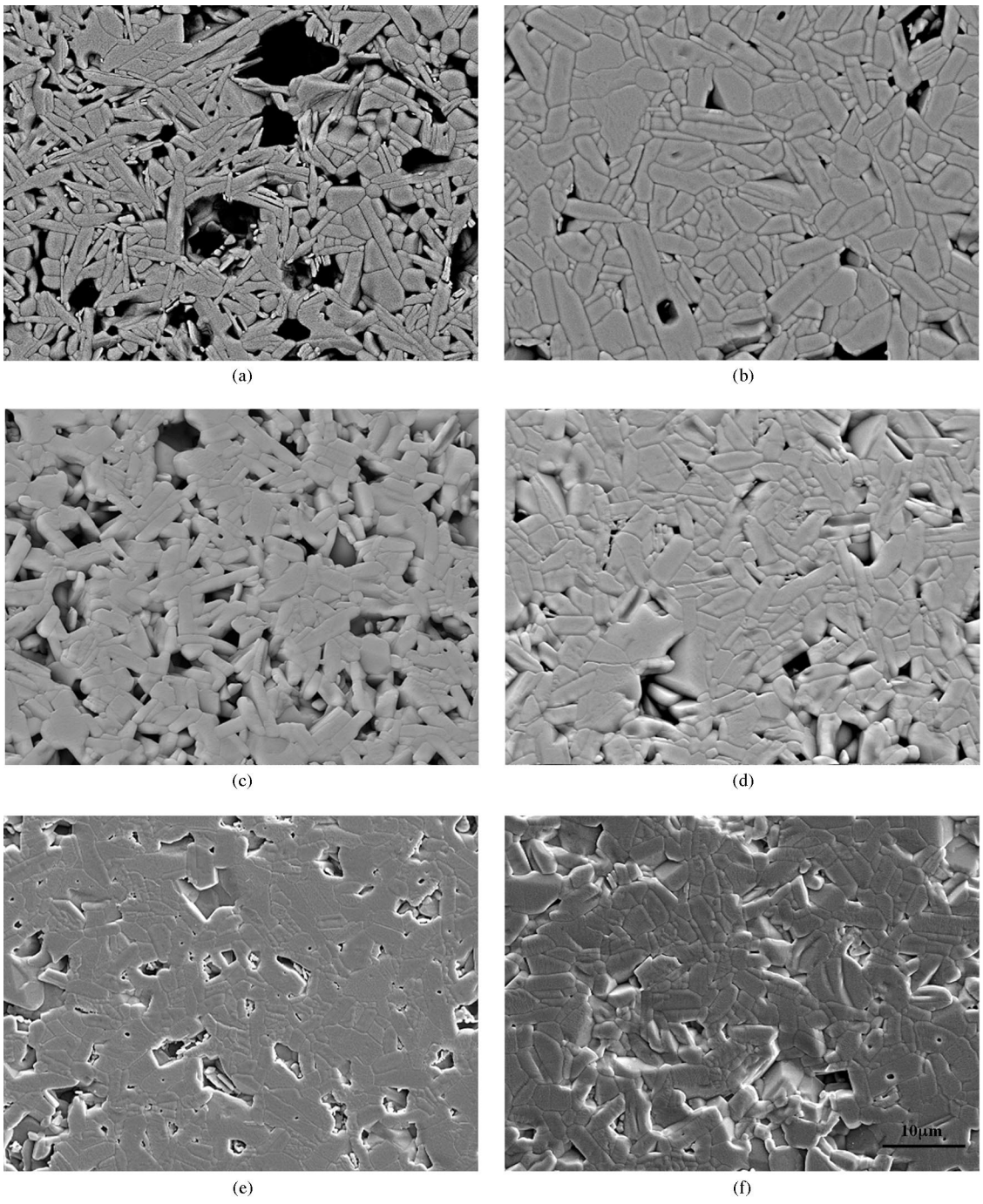

Fig. 2. SEM images of (a) SP, (c) AC and (e) AP samples fired at 1650°C and (b) SP, (d) AC and (f) AP samples fired at 1750°C. Note the higher aspect ratio of (a) in comparison with the other samples.

reported previously. Platelet grains are obtained only in low density and large pore samples, resulting from agglomeration during processing.

These results can be explained by means of a simple reaction mechanism. The mechanism of formation and growth of CA_6 grains from alumina and calcium carbonate powders is schematically depicted in Figs. 4 and 5, in the case of an agglomerated material and a well-dispersed material respectively. After the formation of calcium dialuminate from the reaction between the raw materials, hibonite nucleation occurs at calcium dialuminate–alumina interfaces. Agglomeration diminishes the number of contact areas between alumina and calcium carbonate and therefore between alumina and calcium dialuminate, the number of CA_6 nuclei formed per volume unit varying in the same way. As the reaction progresses, hibonite grains grow along their basal plane and with this plane oriented perpendicular to the

reaction surface. This growth continues until the platelet grains impinge upon each other. When the grain number per volume unit is low, and when sample porosity and pores size are high (see Fig. 4), hibonite grains have enough space to develop with high aspect ratios. On the other hand, when raw materials are well-dispersed, samples are denser and have small pores (see Fig. 5), and CA_6 grains find their rapid growth direction bounded by other hibonite grains before being able to develop high aspect ratios. As reaction progresses, grain growth proceeds in other directions giving grains with lower aspect ratios and curved boundaries. Song and Coble[16,36] have observed a similar behavior during the growth of doped alumina platelike grains.

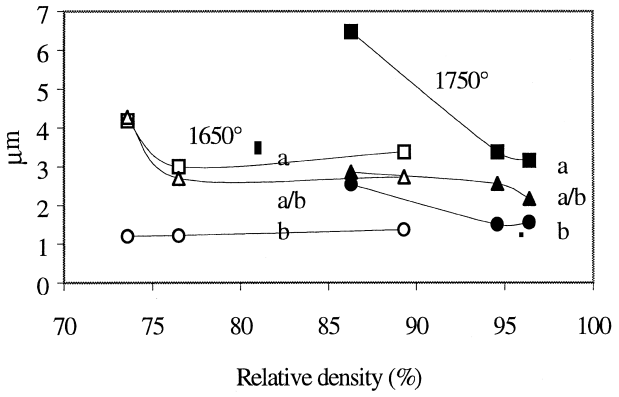

Fig. 3. Final granulometry as a function of relative density and firing temperature. *a* is the length, *b* is the width and *a*/*b* the aspect ratio.

As a consequence, it can be reported that the grain morphology is linked to calcium carbonate and alumina distribution in green specimens. Low green densities promote platelet CA_6 grains while high densities lead to the formation of elongated grains.

Fig. 6 clearly illustrates how grain growth is clamped by the presence of neighboring grains.

Different authors[8,14] proposed that a transient liquid phase, formed during the reaction between $CaCO_3$ and Al_2O_3 to form CA_6, is responsible for the formation of platelet or platelike grains. This liquid phase, if it really appears during the formation of CA_6 grains, is not the only determining factor in microstructural development because, as is shown, platelet CA_6 grains cannot be formed if they have insufficient free space to develop in their preferential grown direction.

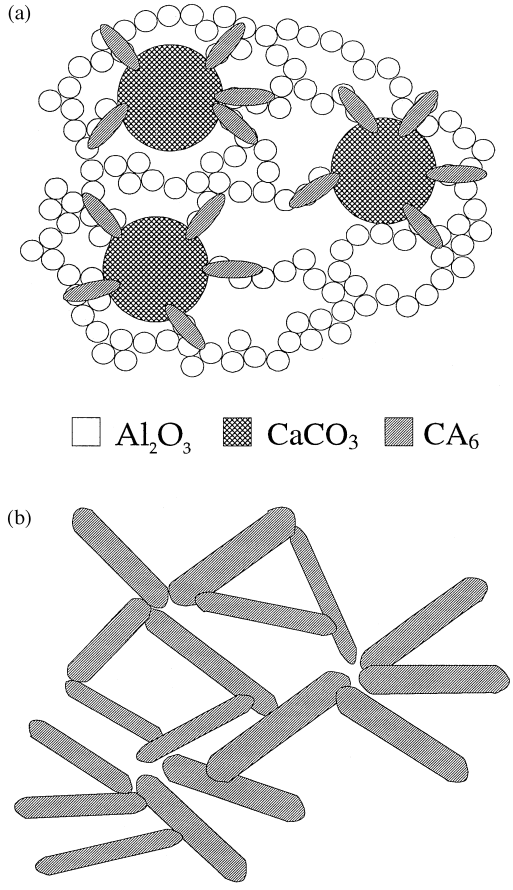

Fig. 4. Schematic representation of the texture development of reaction-sintered calcium hexaluminate grains when the raw materials are agglomerated.

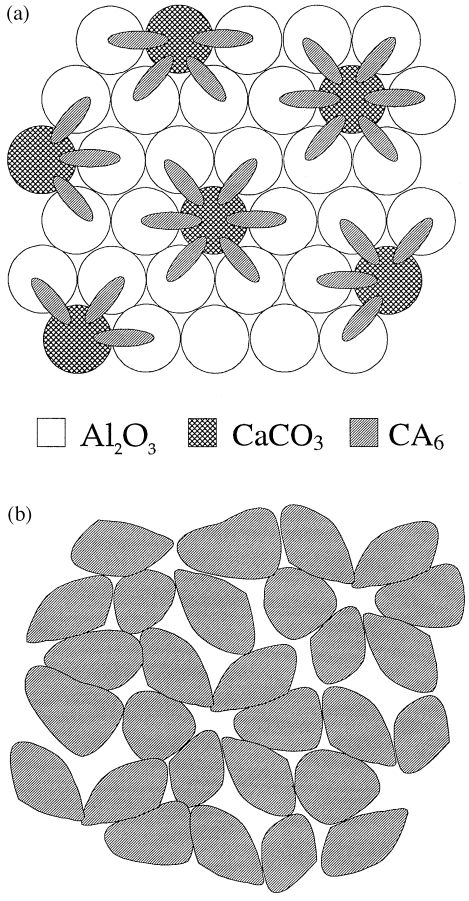

Fig. 5. Schematic representation of the texture development of reaction-sintered calcium hexaluminate grains when the raw materials are well dispersed.

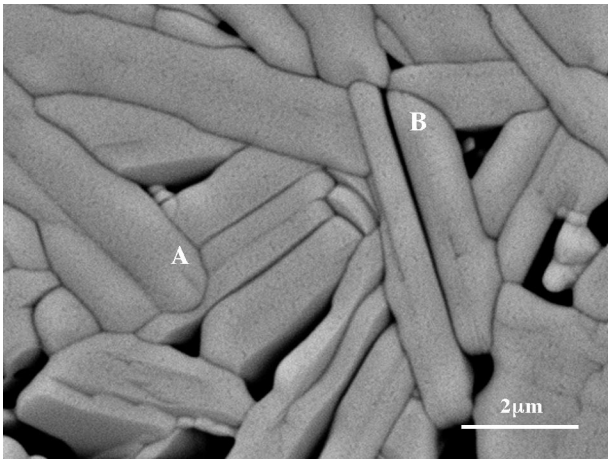

Fig. 6. SEM micrography at high magnification of SP sample fired at 1650°C showing (A) how growth is clamped by the neighboring grains and (B) how the grains weld when they are disposed with their basal plane parallel and stuck together.

After forming, CA_6 grains can grow. The main mechanism responsible for grain growth is the welding of neighboring grains when these are disposed with their basal planes parallel. It can be clearly seen in Fig. 6 how some of these boundaries begin to disappear giving more equiaxed grains.

5. Conclusions

A model has been proposed for the formation of equiaxed or platelike calcium hexaluminate grains. Initial grain distribution, which leads to a variation of porosity and contact area between alumina and calcium carbonate grains, determines final microstructure. A high agglomeration, which promotes a high porosity and low contact area, leads to plate formation. On the contrary, good dispersion promotes low porosity and high contact area that leads to the formation of more equiaxed grains.

An increase of firing temperature, from 1650 to 1750°C, does not much affect grain granulometry except in platelet grains. In this case, grains grow and become more equiaxed as firing temperature increases.

The principal mechanism responsible for this grain growth is the welding of neighbor grains when they are disposed with their basal planes parallel.

References

1. Nurse, R. W., Welch, J. H. and Majumdar, A. J., The CaO–Al_2O_3 system in a moisture-free atmosphere. *Trans. Br. Ceram. Soc.*, 1965, **64**, 409–418.
2. Hallstedt, B., Assessment of the CaO–Al_2O_3 system. *J. Am. Ceram. Soc.*, 1990, **73**, 15–23.
3. Utsunomiya, A., Tanaka, K., Morikawa, H., Marumo, F. and Korima, H., Structure refinement of $CaO{\cdot}6Al_2O_3$. *J. Solid State Chem.*, 1988, **75**, 197–200.
4. Collongues, R., Gourier, D., Kahn-Harari, A., Lejus, A. M., Thery, J. and Vivien, D., Magnetoplumbite related oxides. *Annu. Rev. Mater. Sci.*, 1990, **20**, 51–82.
5. Park, J. G. and Cormack, A. N., Potential models for multicomponent oxides — hexa-aluminates. *Philos. Mag. B*, 1996, **73**, 21–31.
6. Dominguez, C. and Torrecillas, R., Influence of Fe^{3+} in the sintering and microstructural evolution of reaction sintered calcium hexaluminate. *J. Eur. Ceram Soc.*, 1998, **18**, 1373–1379.
7. Criado, E., Estrada, D. A. and de Aza, S., Estudio dilatometrico sobre la formación de dialuminato y hexaluminato de calcio en cementos y hormigones refractarios (dilatometric study of the formation of CA_2 and CA_6 in cements and refractories). *Bol. Soc. Esp. Ceram*, 1976, **15**, 319–321.
8. An, L., Chan, H. M. and Soni, K. K., Control of calcium hexaluminate grain morphology in in-situ toughened ceramic composites. *J. Mat. Science*, 1996, **31**, 3223–3229.
9. Asmi, D. and Low, I. M., Physical and mechanical characteristics of in-situ alumina/calcium hexaluminate composites. *J Mat. Science Lett.*, 1998, **17**, 1735–1738.
10. Kohatsu, I. and Brindley, G. W., Solid state reactions between CaO and α- Al_2O_3. *Z. Phys. Chem., Neue Folge*, 1968, **60**, 79–89.
11. De Jonghe, L. C., Schmidt, H. and Chang, M., Interaction between Al_2O_3 and a CaO–Al_2O_3 melt. *J. Am. Ceram. Soc.*, 1984, **67**, 27–30.
12. de Aza, A., Pena, P. and Moya, J. S., Reactive coating of dolomite on alumina substrates. *J. Eur. Ceram. Soc.*, 1997, **17**, 935–941.
13. Moya, J. S., de Aza, A. H., Steier, H., Requena, J. and Pena, P., Reactive coating on alumina substrates — calcium and barium hexaluminates. *Scrip. Metall. Mat*, 1994, **31**, 1049–1054.
14. Criado, E., Pena, P. and Caballero, A., Influence of processing method on microstructural and mechanical properties of calcium hexaluminate compacts. In *Science of Ceramics, Vol. 14, Proceedings of the 14th International Conference Science of Ceramics*, ed. D. Taylor. Inst. of Ceramics, Shelton, Staffs, UK, 1988, pp. 193–198.
15. Nagaoka, T., Kanzaki, S. and Yamaoka, Y., Mechanical properties of hot-pressed calcium hexaluminate ceramics. *J. Mat. Science Lett.*, 1990, **9**, 219–221.
16. Song, H. and Coble, R. L., Origin and growth kinetics of platelike abnormal grains in liquid-phase-sintered alumina. *J. Am. Ceram. Soc.*, 1990, **73**, 2077–2085.
17. Mendoza, J. L., Freese, A. and Moore, R. E., Thermomechanical behaviour of calcium aluminate composites. In *Ceramic Transactions vol. 4, Advances in Refractories Technology*, ed. R. E. Fisher. American Ceramic Society, Westerville, OH, 1989, pp. 294–311.
18. An, L., Chan, H. M., Padture, N. P. and Lawn, B. R., Damage-resistant alumina-based layer composites. *J. Mater. Res.*, 1996, **11**, 204–210.
19. An, L. and Chan, H. M., R-Curve behavior of in-situ-toughened Al_2O_3:$CaAl_{12}O_{19}$ ceramic composites. *J. Am. Ceram. Soc.*, 1996, **79**, 3142–3148.
20. Criado, E., Caballero, A. and Pena, P., Microstructural and mechanical properties of alumina-calcium hexaluminate composites. In *High Tech Ceramics*, ed. P. Vincenzini. Elsevier Science publishers, Amsterdam, 1987, pp. 2279–2289.
21. Fuhrer, M., Hey, A. and Lee, W. E., Microstructural evolution in self-forming spinel/calcium aluminate-bonded castable refractories. *J. Europ. Ceram. Soc.*, 1998, **18**, 813–820.
22. Buist, D. S., A study of calcium hexaluminate. *Mineralogical Mag*, 1968, **36**, 676–686.
23. Chan, C. and Jo, Y., Effect of CaO Content on the hot strength of alumina-spinel castables in the temperature range of ° to 1500°C. *J. Am. Ceram. Soc.*, 1000, **81**, 19982957–2960.
24. Dayal, R. R. and Glasser, F. P., Phase relations in the system CaO-Al_2O_3-Fe_2O_3. In *Science of Ceramics, vol. 3*, ed. G. H. Stewart. Academic Press, New York, 1967, pp. 191–214.

25. Lister, D. H. and Glasser, F. P., Phase relations in the system CaO–Al_2O_3–iron oxide. *Trans Brit. Ceram. Soc*., 1967, **66**, 293–305.
26. Imlach, J. A. and Glasser, F. P., Sub-solidus phase relations in the system CaO–Al_2O_3–Fe–Fe_2O_3. *Trans. J. Br. Ceram. Soc*., 1971, **70**, 227–234.
27. Tak, J. B. and Young, D. J., Sulfur corrosion of calcium aluminate bonded castables. *Ceram. Bull*, 1982, **61**, 725–727.
28. Cinibulk, M. K. and Hay, R. S., Textured magnetoplumbite fiber–matrix interphase derived from sol–gel fiber coatings. *J. Am. Ceram. Soc*., 1996, **79**, 1233–1246.
29. Cinibulk, M. K., Microstructure and mechanical behavior of an hibonite interphase in alumina-based composites. *Ceram. Eng. Sci. Proc*, 1995, **16**, 633–641.
30. Cinibulk, M. K., Magnetoplumbite compounds as a fiber coating in oxide-oxide composites. *Ceram. Eng. Sci. Proc*, 1994, **15**, 721–728.
31. Arai, H. and Machida, M., Recent progress in high-temperature catalytic combustion. *Catalysis Today*, 1991, **10**, 81–94.
32. Hench, L. L., Clark, D. E. and Harker, A. B., Review nuclear waste solids. *J. Mat. Scien*, 1986, **21**, 1457–1478.
33. Morgan, R. E. D. and Cirlin, E. H., The magnetoplumbite crystal structure as a radwaste host. *J. Am. Ceram. Soc., 65, C*-, 114–115.
34. Morgan, R. E. D., Clarke, D. R., Jantzen, C. M. and Harker, A. B., High-alumina tailored nuclear waste ceramics. *J. Am. Ceram. Soc*., 1981, **64**, 249–258.
35. Halloran, J. W., Role of powder agglomerates in ceramic processing. In *Advances in Ceramics. vol. 9, Forming of Ceramics*, ed. J. A. Mangels and G. L. Messing. American Ceramic Society, Columbus, OH, 1984, pp. 67–75.
36. Song, H. and Coble, R. C., Morphology of platelike abnormal grains in liquid-phase-sintered alumina. *J. Am. Ceram. Soc*., 1990, **73**, 2086–2090.